David Hruschka, Henri Wiedenhoff, Vincent Fleischhauer, Alexander Woyczyk, and Sebastian Zaunseder*

Development of a Dynamic Fluid Phantom -Setup and Validation for an Optical Sensor

https://doi.org/10.1515/cdbme-2025-0157

Abstract: We present a custom fluid phantom usable in the development of sensing technologies to assess the pulse wave. The phantom provides adjustable flow and pressure to an interchangeable target volume and integrates sensors to provide reference readings on fluid dynamics. The proposed system has a modular design and supports the evaluation of various sensing technologies. In this paper, we describe the phantom and demonstrate its basic functionality using the integrated sensors and considering a camera for imaging photoplethysmography as a device under test. Our experiments show reasonable results regarding the performance of the phantom and highlight opportunities for its future use. Due to a wide applicability, easy expansion options and a cost-effective design, we believe that the phantom can contribute to future research activities, not only by our group but even by other groups.

Keywords: fluid phantom, imaging photoplethysmography, PPG, perfusion, camera

1 Introduction

The non-invasive acquisition and processing of pulse waves is a large and very vital field of research. Different sensing principles, e.g. optical, mechanical, or electrical sensors, and processing strategies are in use and still in (further) development. Such developments, particularly those invoking modified sensor setups or novel sensing principles, are often based on experiments involving healthy subjects as starting point. Obviously, the possibilities of introducing variations and even recording a gold standard in healthy subjects are often limited. Physical phantoms offer an opportunity to test functional

David Hruschka, University of Augsburg, Chair for Diagnostic Sensing, Augsburg, Germany, e-mail: david.hruschka@uni-a.de Henri Wiedenhoff, Dortmund University of Applied Science and Arts, Dortmund, Germany, e-mail: henri.wiedenhoff@outlook.de Vincent Fleischhauer, University of Augsburg, Chair of Neurorehabilitation, Augsburg, Germany, e-mail: vincent.fleischhauer@med.uni-augsburg.de

Alexander Woyczyk, University of Augsburg, Chair for Diagnostic Sensing, Augsburg, Germany, e-mail: alexander.woyczyk@uni-a.de

*Corresponding author: Sebastian Zaunseder, University of Augsburg, Chair for Diagnostic Sensing, Augsburg, Germany, e-mail: sebastian.zaunseder@uni-a.de

principles and contribute to the development of novel sensing technologies.

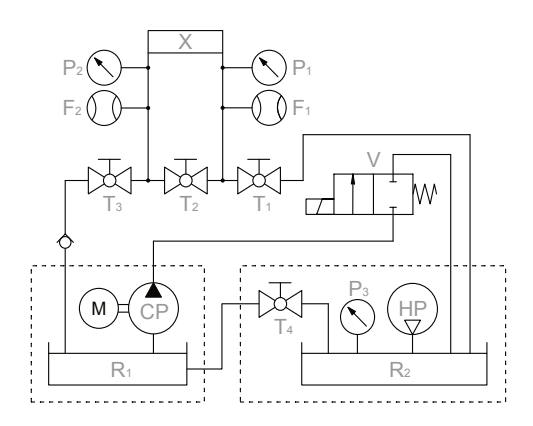
As such a technology, within this work, we focus on optical measurement technologies, namely photoplethy smography (PPG) and particularly imaging PPG (iPPG), i.e. non-contact PPG by a camera. Some works describe physical phantoms in the context of PPG and pulse oximetry. E.g., Bhusal et al. and Rodrigues et al. recently described phantoms to pulse oximetry's assessment [1, 5]. Jenne et al. [2] and Nwafor et al. [4] both proposed phantoms more directed at PPG. Nwafor et al. thereby specifically targeted iPPG and evaluated the ability to capture pulsation as well as to resolve tube structures using their phantom [4]. Although there is some work, the use of phantoms is not yet widespread and existing solutions often invoke costly hardware. Affordable solutions suited for flexible use might contribute to ongoing research activities by providing experimental facilities to a larger community.

This contribution presents a fluid phantom that can be used for the development of novel sensing technologies to assess the pulse wave. The work covers a technical description of our phantom in its current state together with a preliminary validation on the exemplary use-case of camera-based perfusion assessment.

2 Material and Methods

2.1 Overview

The phantom aims to provide an adjustable pressure/flow to a target volume and supports real-time measurements of fluid dynamics. The target volume is interchangeable to mimic different parts of the circulation and assess the function of variable sensing technologies and devices under test (DUT), respectively. The remaining system, which includes fluidic components, sensors, the control system and additional hardware for data acquisition, is designed for generalized use with variable target volumes. In the following, we first provide a description of this general part. Afterwards, we detail the specific setup for this study, i.e. the target volume used and the experiments for this contribution.



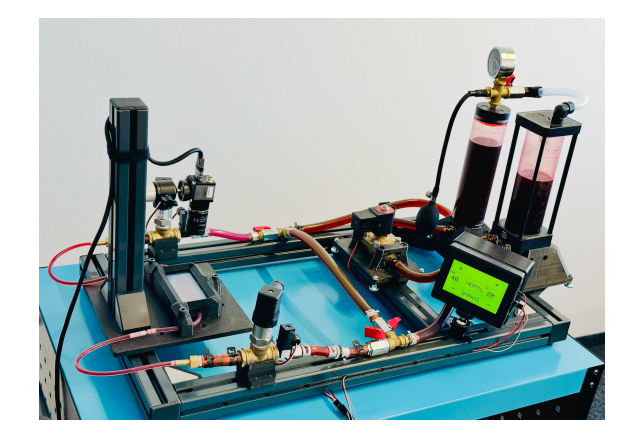


Fig. 1: Illustration of the used phantom. Left: Schematic of the implemented fluid circulation. X is the target volume to be perfused. $P_{1,2}$ and $F_{1,2}$ are electronic pressure and flow sensors. P_3 is a mechanical manometer. P_4 are fluid reservoirs. P_4 is the centrifugal fluid pump. HP is a hand air pump to adjust the pressure level. P_4 are manually operated ball valves (in this work, P_4 is completely closed, P_4 are (partially) open). V is an actuated valve. Peripheral components (data acquisition, control unit, display) are not shown. Right: Photo of the phantom.

2.2 General setup

Fig. 1 illustrates the phantom. Below, we provide further details on the fluidic components, the control and the integrated sensors as well as signal acquisition.

Fluidic components: To drive the fluid we use the centrifugal pump (CP) Alphacool VPP655PWM Single Edition (Alphacool International GmbH; Braunschweig, Germany). Two reservoirs Alphacool Eisbecher Aurora D5 250 mm (Alphacool International GmbH; Braunschweig, Germany) ensure the supply of water (R1) and serve to buffer pulsation (R2). Pulsatile flow is generated by the 2/2-way valve normally closed solenoid valve RSV01 (Rotork plc; Bath, UK). In addition, there are four brass ball valves Mini PN 16 (MT Business Key S. L.; Pallejà, Spain), which are static throughout the experiment. As connectors, we use PVC tubes with an inner diameter of 12 mm.

Control: The dynamic behavior of the phantom is controlled using an Arduino Giga R1 WiFi. Currently, pulse rate (PR) and duty cycle (DT) of valve V can be adjusted via an integrated touch screen (Giga Display Shield). The duty cycle is defined by $DT = \tau_v/T$ where τ_v is the opening time of valve V and T is the duration of the cycle, that is $^{1}/PR$. Note that other parameters, such as the pump outflow, can also be adjusted in the software, but this is beyond the scope of this contribution.

Sensors and signal acquisition: We integrated two electronic pressure transmitters DT1 G1/2" with measuring range of -1.0 bar to 0.6 bar (otom Group GmbH; Bräunlingen, Germany) and two turbine flow meters with measuring range $0.11/\min - 2.01/\min$ (Badger Meter Europa GmbH; Neuffen, Germany). The sensors are placed right before and after the target volume. Sensor data is fed into a Biopac MP160 data acquisition unit (Biopac; Goleta, United States of America),

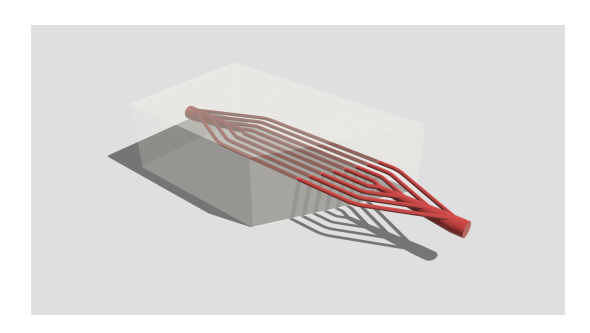
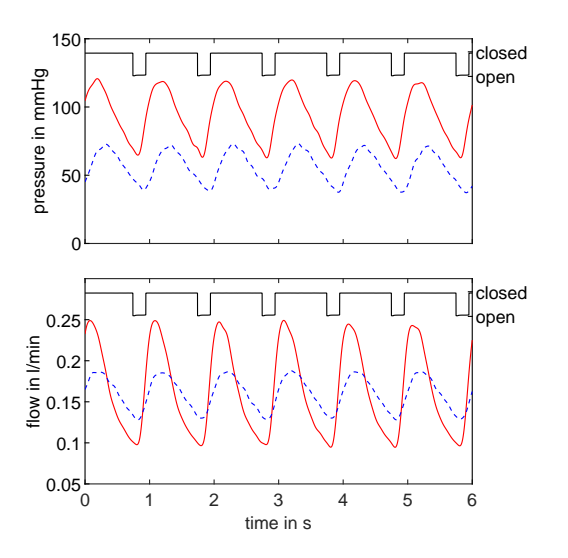


Fig. 2: Cut through the tissue phantom used in this work (we use two phantoms with tube widths of $1.0\,\mathrm{mm}$ and $0.8\,\mathrm{mm}$ and adjusted spacing between tubes). Red parts show the sacrificial material, i.e. tubes, embedded in the silicone corpus. During manufacturing, the sacrificial material was connected to external tubes before casting the corpus.

which serves as data acquisition, real-time visualization, and storage system. While pressure sensors provide an analogue voltage that is proportional to pressure, flow meters provide a pulse frequency modulated signal, which is then converted to flow. To illustrate the function of the valve, its state is also fed into the data acquisition system.

2.3 Case-specific setup

Target volume and fluid: As target volumes within this work, we designed two tissue phantoms with integrated tube structures to mimic superficial vessels. Both tissue phantoms have an equal size of approx. $90 \, \mathrm{mm} \times 40 \, \mathrm{mm} \times 20 \, \mathrm{mm}$ (length x width x depth). There are differences in their tube sizes $(1.0 \, \mathrm{mm} \, \mathrm{vs.} \, 0.8 \, \mathrm{mm})$ and tube distances $(1.7 \, \mathrm{mm} \, \mathrm{vs.} \, 0.8 \, \mathrm{mm})$. In either tissue phantom, the vessel structure is located at an approximate depth of $8.5 \, \mathrm{mm}$. As base material for the tissue phantoms, we employ silicone resulting in a slightly tur-



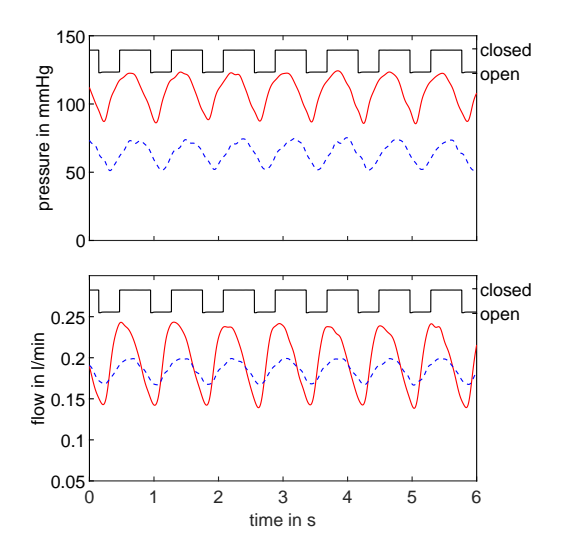


Fig. 3: Phantom signals using the target volume with structure size of $1.0\,\mathrm{mm}$ (at PR= $60\,\mathrm{bpm}$ and DT= $20\,\%$) and with structure size of $0.8\,\mathrm{mm}$ (at PR= $75\,\mathrm{bpm}$ and DT= $40\,\%$). Upper plots: black - action of valve V; red - pressure by P₁; blue dotted - pressure by P₂. Lower plots: black - action of valve V; red - flow by F₁; blue dotted - flow by F₂. Elements are denoted according to Fig. 1.

bid corpus. The tubes are created in a subtractive process described below. Fig. 2 shows a sketch of a resulting tissue phantom. As fluid in our experiments, we use water with 1/10 part vinegar essence and red food coloring for dyeing.

Fabrication process of the tissue phantom: The fabrication of the tissue phantom begins with the 3D printing of a sacrificial mold that defines the vascular structures. This mold is printed using a water-soluble filament (Ultrafuse BVOH Natural) on a fused deposition modeling (FDM) 3D printer. The outer casting frame, which simultaneously functions as a structural support for the tissue phantom and provides interfaces for the inlet and outlet connections (tubes of inner diameter of 4 mm), is also fabricated via FDM using polyethylene terephthalate glycol (PolyLite PETG). A two-component silicone (Premium 200 Silicone – Transparent) is thoroughly mixed and subsequently degassed under vacuum at -1 bar to remove trapped air and reduce the formation of air bubbles. The degassed silicone is then poured into the casting frame, fully embedding the sacrificial mold along with pre-positioned 6 mm silicone tubes at the inlet and outlet port. The inlet and outlet to the tissue phantom are permanently embedded in the silicone during the casting process. After curing for approximately four hours at room temperature, the sacrificial mold is removed by submerging the assembly into a water bath. The dissolution process can be accelerated by increasing the water temperature, applying mild pressure to the fluid connections, and actively flushing the internal structures.

Experiments: Our experiments are intended to prove the basic functions of the phantom and to show opportunities for future use. As an exemplary application, we consider iPPG. The IDS UI-3060CP-C-HQ Rev.2 RGB camera (IDS Imaging

Development Systems GmbH; Obersulm, Germany) serves as DUT. We record RGB videos in daylight at a frame rate of 40 fps, resolution of 840 x 1240 pixels, and color depth of 12 bits per channel. Our experiments include variations in the parameter settings of the phantom, namely two PR (60 bpm and 75 bpm) and two DC (20 % and 40 %). We record data for both tissue phantoms in each parameter setting for $\approx 15\,\mathrm{s}$ and use excerpts from those intervals in our result section. The intervals were taken at phases of stable operation, i.e. transitions between settings are not considered here.

2.4 Data processing

Sensor data from pressure/flow transducers is filtered in forward and backward direction by a 5th order Butterworth low-pass filter with cutoff at 8 Hz.

Considering the video data, we only use the green channel. We manually define a static region of interest (ROI) that covers almost the entire top view of the tissue phantom. For 1D analysis, we extract an iPPG signal by averaging the green channel over the ROI and subtract it from 4095 to yield the common photoplethysmographic waveform. The signal is bandpass filtered in the range of 0.4 Hz - 8 Hz by applying two 5th order Butterworth filters in forward and backward direction. To capture 2D characteristics, we employ lock-in amplification within the ROI similar to [3] to assess the strength of pulsation. Thereto, we first spatially smooth each image using a disk shaped filter with radius of eight pixels. Afterwards, the aforementioned 1D signal processing is applied to single (smoothed) pixel traces, and (using the 1D PPG signal from the ROI as reference) lock-in amplification is used to calculate amplitude maps from a signal excerpt of 10 s.

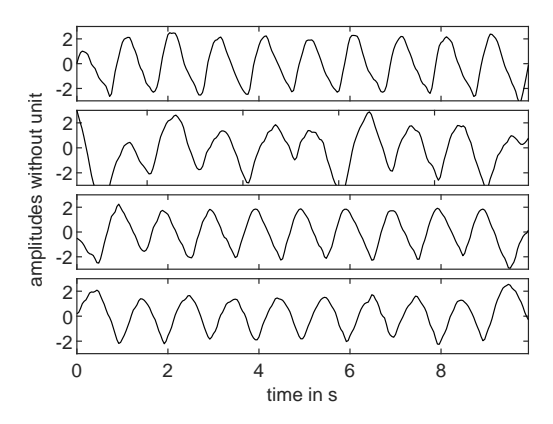


Fig. 4: iPPG signals at PR of $60\,\mathrm{bpm}$. The upper two plots originate from the phantom of tube size of $1\,\mathrm{mm}$, the lower plots from the phantom of tube size $0.8\,\mathrm{mm}$. For each tube size, the upper plot is at a DT of $20\,\%$ and the lower one at $40\,\%$.

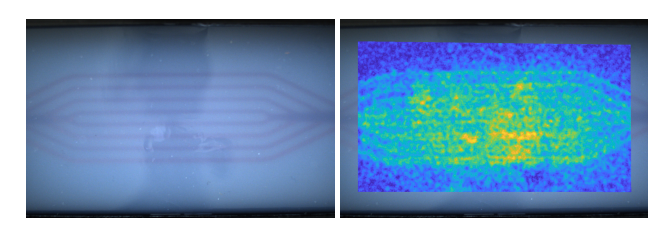


Fig. 5: Spatial assessment of the phantom. Left: Foto of the phantom (single video frame). Right: overlaid pulsation strength in the ROI calculated by lock-in amplification.

3 Experimental results

In the following, we provide exemplary results from our experiments and highlight the most important findings.

Fig. 3 shows phantom signals (pressures, flows and valve action). The behavior reflects our expectation including a pressure drop owing to the tissue phantom's resistance, smoothing of flow, and minor temporal differences between the pressure and flow waves before and after the phantom.

Fig. 4 shows exemplary 1D iPPG signals taken from the ROI under different parameter settings. The signals clearly reflect the pulsating behavior as expected. In addition, there are observable morphological differences between settings. However, there also are disturbances, which introduce large variations hampering morphological analysis.

Finally, Fig. 5 shows a 2D analysis of pulsation using lock-in amplification. As can be seen, a blurred tube structure is forming. Blurring is partly introduced by image preprocessing, i.e. smoothing, but also occurs due to physical effects, i.e. scattering, specular reflection and surface contamination, which hamper the assessment of pulsation. However, despite those effects we are able to retrieve detailed spatial information on the pulsation from the tube structure.

4 Conclusions

Major findings: Our experiments demonstrate the basic function of the proposed phantom. The phantom is a low-cost system that opens up, due to its modular design, far-reaching experimental opportunities relevant to multiple fields of research concerning the assessment of pulse waves. With respect to iPPG, we did not carry out systematic experiments and quantitative analyzes, but included the technique to demonstrate a relevant use case of the phantom. In this regard, our experiments show the feasibility and underline the opportunities for future systematic experiments using the phantom.

Limitations: The presented fluid phantom is in an early stage, and there are aspects that can be improved in the future. An example relates to the setup of absolute pressures and flows: using the available setting, it is difficult to set them precisely. However, the integrated sensors provide pressure and flow measurements that can be used as a reference for subsequent analyzes of a DUT. Owing to the real-time feedback, it is also possible to approach desired values in an experimental manner, but setting up precise values certainly has advantages. A future integration of an automated control loop can resolve the issue without requiring large modifications or additional components. Another limitation refers to the sensors used. Although the current sensors are adequate for the presented experiment, there might be better suited options with regard to resolution and/or dynamic behavior.

Outlook: Future work beyond the use of the phantom in systematic experiments will address the limitations mentioned and introduce selective optimizations. In addition, as stated before, optical recordings are only one use case. A current field of work is the extension to mechanical and electrical sensors.

References

- Anant Bhusal et al. "Development and characterization of silicone-based tissue phantoms for pulse oximeter performance testing." In: *Journal of Biomedical Optics* 29.S3 (2025), pp. 1–19.
- [2] Sophie Jenne and Hans Zappe. "Multiwavelength tissue-mimicking phantoms with tunable vessel pulsation." In: *Journal of Biomedical Optics* 28.04 (2023), pp. 1–13.
- [3] Alexei A Kamshilin et al. "Variability of microcirculation detected by blood pulsation imaging." In: *PloS one* 8.2 (2013), e57117.
- [4] C. Ikenna Nwafor et al. "Assessment of a noninvasive optical photoplethysmography imaging device with dynamic tissue phantom models." In: *Journal of Biomedical Optics* 22.09 (2017), p. 1.
- [5] Andres J. Rodriguez et al. "Tissue mimicking materials and finger phantom design for pulse oximetry." In: *Biomedical Optics Express* 15.4 (2024), p. 2308.